ANALYSIS OF SPECTRAL RADIATION FIELDS IN SCATTERING MATERIALS UNDER EXPOSURE TO DIFFUSE FLUXES DIRECTED AT A CERTAIN ANGLE

S. G. Il'yasov, N. I. Angersbakh, and A. K. Angersbakh

UDC 536.3

Computational formulas are presented, quantities are determined and the change in the spectral composition is illustrated in a three-layer system by the different degree of resultant flux density, spatial irradiance, and absorbed energy for solar radiation and a KG-220-1000 IR generator. An experimental-analytic method of determining the optical and two-hemispherical thermal radiation characteristics of scattering materials is considered by the measured directional-hemispheric reflexivity and transmissivity of a layer of finite thickness.

The establishment of regularities for the solar and IR generator spectral radiation distribution in scattering materials is of great value in connection with the necessity to describe heat and mass transfer during heat treatment and drying under exposure to a diffuse flux directed at a certain angle [1-4].

It is necessary to have data about the spectral magnitudes the spatial irradiance E_{λ_0} the resultant flux density q_λ, the resultant flux density w_λ for a complete representation of the radiation field within a layer of material.

Real scattering materials are systems consisting of several layers that selectively absorb and scatter radiation. To analyze the radiation field, a number of materials (polymer films, paint and varnish coating, plant materials, etc.) can be represented in the form of models consisting of three absorbing and scattering layers: 1) shell, 2) material, 3) shell.

The influence of the effect of multiple boundary reflection on the energy distribution and spectral composition of radiation complicated the analysis considerably. [1, 3]. Thus, in the case of exposure to a broad directional flux it is necessary to take account of the external boundary reflection and the multiple internal reflection from the boundaries of each of the materials (shell, material, and shell) for the non-scattered component of the radiation flux in the layer and the radiation flux component scattered within the layer. The path of the non-scattered component of radiation flux that enters the layer at an angle $\theta = \arccos \mu$ is governed under multiple internal reflection by the laws of geometric optics. The method of taking account of the external and internal reflection effects from the layer boundaries is examined in [1, 3] in detail for the solution of the radiation energy transport differential equations by formulation of the appropriate boundary conditions for the cases of exposure to diffuse fluxes directed at a certain angle to an individual layer and to a multilayered system. Taking account of multiple reflections between layers of the shell and the remaining system, the material + shell, to determine the radiation flux entering the material layer can be realized by using the coefficient $M_{i,\ j}$ [1-3]

$$E'_{\lambda 1} = E'_{\lambda 1 \text{п}} T'_0 M_{1,(2+3)}\ ;\ E'_{\lambda 2} = E'_{\lambda 2 \text{п}} T'_0 M_{3,(2+1)}\ . \tag{1}$$

The effects of the external and internal boundary reflection of the radiation in the shell layer are taken into account in a natural manner in the experimental determination of the shell spectral characteristics R'_0 and T'_0 and the computations are simplified. In many

Moscow Technological Institute of the Food Industry. Translated from Inzhenerno-Fizicheskii Zhurnal, Vol. 58, No. 4, pp. 663-670, April, 1990. Original article submitted May 4, 1987.

0022-0841/90/5804-0507$12.50

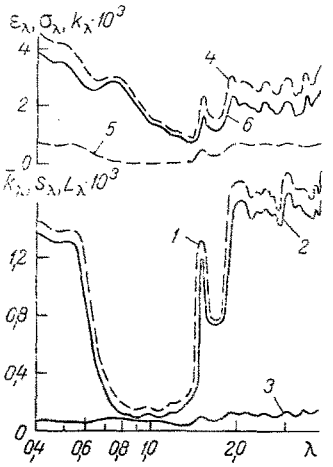

Fig. 1. Spectral optical characteristics of grapes 1) L_λ; 2) $\bar{k}_\lambda$; 3) s_λ; 4) ε_λ; 5) k_λ; 6) σ_λ, ε_λ, σ_λ, k_λ, $\bar{k}_\lambda$, s_λ, L_λ, m^{-1}; λ, μm.

radical cases $R_0' < 0.1$ for the shell and $R_\lambda' < 0.5$ for the layer and taking account of multiple reflections between the shell and material layers for engineering computations will hardly be substantial ($R_1 R_{(2+3)} < 0.05$, $M_{1,\,(2+3)} > 0.95$).

It was shown in [2] that to simplify the analysis of radiation energy transfer in such cases the shell (because of its small thickness) can be taken as the boundary under directional irradiation that reflects, absorbs, and transmits radiation, and it can be assumed that radiation fluxes pass through it whose densities equal $E_1'T_0'$ and $E_2'T_0'$. Computational formulas are presented in [2] to determine the magnitude of the absorbed energy flux w_λ' under exposure to diffuse fluxes directed at a certain angle and the adequacy is shown of the model selected in a specific example of a three-layer system. We present computational formulas for $E_{\lambda 0}'$ and q_λ'.

In the case of bilateral exposure to radiation fluxes directed at certain angles q_λ' with densities $E_{\lambda 1\Pi}'$ and $E_{\lambda 2\Pi}'$, the magnitude of the resultant flux $\Theta = \arccos \mu$ is determined from the expression

$$
\begin{aligned}
q_\lambda' = {} & E_{\lambda 1}' T_0' \frac{1 - R_{\lambda\infty}}{1 - \Psi_\lambda^2} \left\{ C_2 \left[\exp(-L_\lambda x) + \frac{\Psi_\lambda^2}{R_{\lambda\infty}} \exp(L_\lambda x) \right] - \right. \\
& - C_1 \exp\left(-\frac{\varepsilon_\lambda}{\mu} l\right) \left. \left[\exp[-L_\lambda (l - x)] + \frac{\Psi_\lambda^2}{R_{\lambda\infty}} \exp[L_\lambda (l - x)] \right] \right\} + \\
& + (1 + C_1 - C_2) E_{\lambda 1}' T_0' \exp\left(-\frac{\varepsilon_\lambda}{\mu} x\right) - \\
& - E_{\lambda 2}' T_0' \frac{1 - R_{\lambda\infty}}{1 - \Psi_\lambda^2} \left\{ C_2 \left[\exp[-L_\lambda (l - x)] + \frac{\Psi_\lambda^2}{R_{\lambda\infty}} \exp[L_\lambda (l - x)] \right] - \right. \\
& - C_1 \exp\left(-\frac{\varepsilon_\lambda}{\mu} l\right) \left. \left[\exp(-L_\lambda x) + \frac{\Psi_\lambda^2}{R_{\lambda\infty}} \exp(L_\lambda x) \right] \right\} - \\
& - E_{\lambda 2}' T_0' (1 + C_1 - C_2) \exp\left[-\frac{\varepsilon_\lambda}{\mu} (l - x)\right],
\end{aligned}
\tag{2}
$$

where

$$\Psi_\lambda = R_{\lambda\infty} \exp(-L_\lambda l). \tag{3}$$

The magnitude of the spatial irradiance equals

$$E'_{\lambda 0} = E'_{\lambda 1} T'_0 \frac{1+R_{\lambda\infty}}{1-\Psi_\lambda^2}\left\{C_2\left[\exp(-L_\lambda x) - \frac{\Psi_\lambda^2}{R_{\lambda\infty}} \exp(L_\lambda x)\right] + \right.$$
$$+ C_1 \exp\left(-\frac{\varepsilon_\lambda}{\mu} l\right)\left.\left[\exp[-L_\lambda(l-x)] - \frac{\Psi_\lambda^2}{R_{\lambda\infty}} \exp[L_\lambda(l-x)]\right]\right\} -$$
$$- E'_{\lambda 1} T'_0 (C_1 + C_2 - 1) \exp\left(-\frac{\varepsilon_\lambda}{\mu} x\right) +$$
$$+ E'_{\lambda 2} T'_0 \frac{1+R_{\lambda\infty}}{1-\Psi_\lambda^2}\left\{C_2\left[\exp[-L_\lambda(l-x)] - \frac{\Psi_\lambda^2}{R_{\lambda\infty}} \exp[L_\lambda(l-x)]\right] + \right.$$
$$+ C_1 \exp\left(-\frac{\varepsilon_\lambda}{\mu} l\right)\left.\left[\exp(-L_\lambda x) - \frac{\Psi_\lambda^2}{R_{\lambda\infty}} \exp(L_\lambda x)\right]\right\} -$$
$$- E'_{\lambda 2} T'_0 (C_1 + C_2 - 1) \exp\left[-\frac{\varepsilon_\lambda}{\mu}(l-x)\right]. \tag{4}$$

In an optically infinitely thick layer ($L_\lambda l \to \infty$, $\varepsilon_\lambda l \to \infty$) the magnitudes of the total flux density vector, spatial irradiance, and absorbed energy equal

$$q'_\lambda = E'_\lambda T'_0 (1 - R_{\lambda\infty}) C_2 \exp(-L_\lambda x) + (1 + C_1 - C_2) E'_\lambda T'_0 \exp\left(-\frac{\varepsilon_\lambda}{\mu} x\right), \tag{5}$$

$$E'_{\lambda 0} = E'_\lambda T'_0 \left[(1 + R_{\lambda\infty}) C_2 \exp(-L_\lambda x) - (C_1 + C_2) \exp\left(-\frac{\varepsilon_\lambda}{\mu} x\right)\right] +$$
$$+ E'_\lambda T'_0 \exp\left(-\frac{\varepsilon_\lambda}{\mu} x\right), \tag{6}$$

$$W'_\lambda = \bar{k}_\lambda E'_\lambda T'_0 \left[(1 + R_{\lambda\infty}) C_2 \exp(-L_\lambda x) - (C_1 + C_2) \exp\left(-\frac{\varepsilon_\lambda}{\mu} x\right)\right] +$$
$$+ k_\lambda E'_\lambda T'_0 \exp\left(-\frac{\varepsilon_\lambda}{\mu} x\right). \tag{7}$$

The presented solutions (2)-(7) differ from the general solutions [1, 3] in that the magnitude of the shell transmissivity T'_0 being determined, in which information is also contained about its reflecting and absorbing properties

$$T'_0 = 1 - (R'_0 + A'_0).$$

is taken into account.

The method published in [1-3] is used to compute the radiation fields in scattering materials under exposure to diffuse flux.

The magnitudes of the optical k_λ, $\bar{k}_\lambda$, L_λ, ε_λ and bihemispherical thermoradiational $R_{\lambda\infty}$ characteristics as well as the Duntley parameters C_1 and C_2 which are not subject to direct

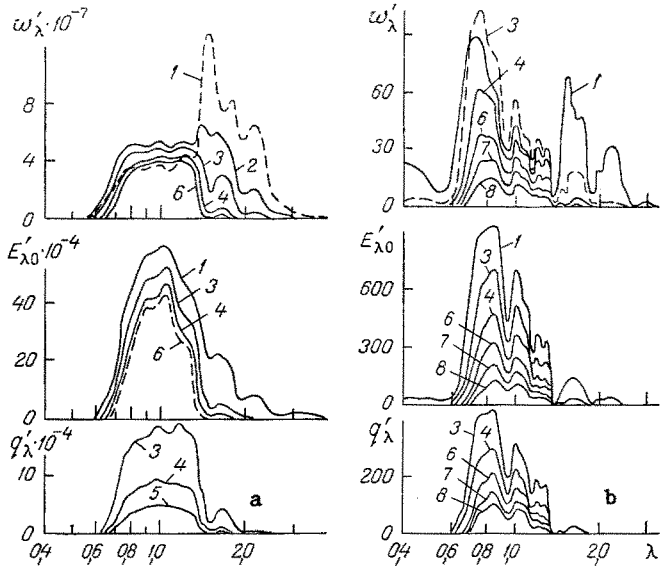

Fig. 2. Change in the spectral composition of IR-generator (a) and solar (b) radiation in a grape berry layer under directional exposure at a different depth: 1) x = 0 mm; 2) 1; 3) 2; 4) 4; 5) 5; 6) 6; 7) 8; 8) 10 mm; a) bilateral nonsymmetric exposure $E_2 = 0.8 \cdot E_1$; b) unilateral exposure $E_2 = 0$, w'_λ, Bt/m^3; $E'_{\lambda 0}$, q'_λ, Bt/m^2.

measurement but are expressed in terms of the optical characteristics, enter into (2)-(7) for computation of the radiation fields in scattering materials (capillary-porous, colloidal, polymer, etc.) under directional exposure.

The Duntley parameters C_1 and C_2 are associated with the fundamental and averaged optical characteristics [1, 3]

$$C_1 = \frac{\mu s' \varepsilon_э - s' \varepsilon + \mu f' s}{\varepsilon^2 - \mu^2 L^2}, \tag{8}$$

$$C_2 = \frac{\mu f' \varepsilon_э + f' \varepsilon + \mu s' s}{\varepsilon^2 - \mu^2 L^2}, \tag{9}$$

where

$$\varepsilon_э = \bar{k} + s, \ \varepsilon = k + \sigma, \ L = \sqrt{\bar{k}(\bar{k} + 2s)}. \tag{10}$$

Knowing the layer R'_λ and T'_λ under directional exposure, the C_1 and C_2 can be determined from a nomogram [8], hence the coefficients $\bar{k}_\lambda$ and s_λ are determined. Information about the indicatrix $\chi_\lambda(\gamma)$ and the angular distribution of the radiation intensity $B_\lambda(\Theta, \omega')$ is taken into account in $\bar{k}_\lambda$ and s_λ by using the spatial distribution coefficient of the incident radiation flux $m(1 < m < \infty)$ and the coefficients δ_s, δ_f [1, 3]

$$s = \delta_s \sigma m, \ f = \delta_f \sigma m, \ s' = \delta_s \sigma, \ f' = \delta_f \sigma, \ \bar{k} = mk. \tag{11}$$

The mode of the indicatrix is taken into account by using the coefficients δ_s and δ_f that are numerically equal to fractions of the whole "backscattered" and "forward" scattered by a volume element or layer upon exposure to radiation flux in the solid angle $w' \leq 2\pi$ with the angular intensity distribution $B_\lambda(\Theta, \omega')$. The quantities δ_s and δ_f vary within the limits $0 < \delta_s < 1$ and $0 < \delta_f < 1$, and their sum here equals $\delta_s + \delta_f = 1$.

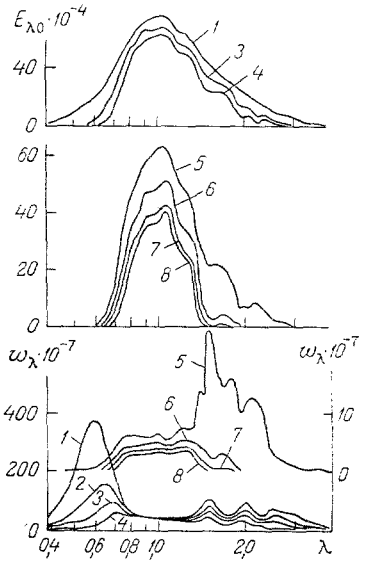

Fig. 3. Change in the spectral composition of IR-generator radiation in a shell (curve 1-4) and in a layer (curves 5-8) of grape berries under diffuse exposure at a different depth 1) x = 0 mm; 2) 0.05; 3) 0.1; 4) 0.2; 5) 0; 6) 2; 7) 4; 8) 6 mm. E_{λ_0}, Bt/m^2; w_λ, Bt/m^3.

The optical characteristics are determined by using experimental data on R_λ, T_λ and $R_{\lambda\infty}$ under diffuse exposure

$$L_\lambda = \frac{1}{l} \ln \left(\frac{1 - R_\lambda R_{\lambda\infty}}{T_\lambda} \right), \tag{12}$$

$$\overline{k}_\lambda = \frac{1 - R_{\lambda\infty}}{1 + R_{\lambda\infty}} L_\lambda, \quad s_\lambda = \frac{2R_{\lambda\infty}}{1 - R_{\lambda\infty}^2} L_\lambda. \tag{13}$$

The external parameters, the directionally hemispherical reflexivity R'_λ and transmissivity T'_λ of a finite thickness layer [1] measured under direction exposure, are most accessible to experimental determination. Establishment of a connection between the substance internal parameters and the layer external parameters is a difficult and not always solvable problem. Experimental-analytic and graphical methods of determining the fundamental radiation field characteristics in light scattering materials have been developed in a number of papers [1, 3, 5-9], based on the mutual relation between the optical and bihemispherical thermoradiational characteristics of the layer, whose application is possible for our case but is difficult and they do not permit determination of all the quantities entering into (3)-(7). In this connection, an experimental-analytic method of determining the optical and thermoradiational characteristics is proposed and realized on an electronic computer. Underlying this method is the Duntley idea of a graphical determination of the characteristics [8].

Applying the substitution $z = \exp(-L_\lambda \ell)$ and starting from the analytic solution of the system of equation relating the four unknown quantities R_λ, T_λ, C_1 and C_2 to the experimentally determinable thermoradiation characteristics R'_λ and T'_λ (in the case $\exp(-\varepsilon_\lambda \ell) \ll T_\lambda$ [1, 3]) for specimens of two different thicknesses ℓ_1 and ℓ_2:

$$R'_\lambda = C_2 R_\lambda - C_1, \quad T'_\lambda = C_2 T_\lambda, \tag{14}$$

we obtain computational formulas for $R_{\lambda\infty}$, L_λ, z_λ:

$$R_{\lambda\infty} = \frac{R_\lambda + T_\lambda - z_\lambda}{1 - (R_\lambda + T_\lambda) z_\lambda}, \tag{15}$$

$$L_\lambda = -\frac{1}{l} \ln z_\lambda, \tag{16}$$

$$z_\lambda = \frac{(1 + T_\lambda^2 - R_\lambda^2) - \sqrt{(1 + T_\lambda^2 - R_\lambda^2) - 4T_\lambda^2}}{2T_\lambda}. \tag{17}$$

The quantities R'_λ and T'_λ, measured under directional radiation for the two specimens with $\ell_1 \neq \ell_2$, are used as bihemispheric R_λ and T_λ in a first approximation to compute the values of $R_{\lambda\infty H}$, $L_{\lambda 1H}$, $z_{\lambda 1H}$ for a specimen of thickness ℓ_1 from (15)-(17). A refined computation is then performed according to the following method.

By using the quantities $L_{\lambda 1H}$ and $R_{\lambda\infty H}$ in the first approximation, we calculate the thermoradiational characteristics of the second layer of thickness ℓ_2 by the Duntley method [8]:

$$T_{\lambda 2H} = \frac{(1 - R^2_{\lambda\infty H}) \exp(-L_{\lambda 1H} l_2)}{1 - R^2_{\lambda\infty H} \exp(-2L_{\lambda 1H} l_2)}, \tag{18}$$

$$R_{\lambda 2H} = R_{\lambda\infty H} \frac{1 - \exp(-2L_{\lambda 1H} l_2)}{1 - R^2_{\lambda\infty H} \exp(-2L_{\lambda 1H} l_2)}. \tag{19}$$

Comparing the magnitudes of the experimental $T'_{\lambda 2H}$ and $R_{\lambda 2H}$ with the magnitudes C_1 and C_2 computed by means of (18) and (19) by analogy with the Duntley method [8], we find the values of the parameters C_1 and C_2 (in the case of $\exp(-\varepsilon_\lambda \ell) \ll T_\lambda$):

$$C_2 = \sqrt{\frac{T'_{\lambda 2}}{T_{\lambda 2H}}}, \tag{20}$$

$$C_1 = \frac{1}{2}(R_{\lambda 2H} - R'_{\lambda 2}) C_2. \tag{21}$$

By means of the values found for the Duntley parameters C_1 and C_2 we determine the desired bihemispheric thermoradiational characteristics of the layers ℓ_1 or ℓ_2:

$$R_\lambda = \frac{R'_\lambda + C_1}{C_2}, \quad T_\lambda = \frac{T'_\lambda}{C_2}. \tag{22}$$

Using the quantities R_λ and T_λ, we calculate the desired values of z_λ, L_λ, $R_{\lambda\infty}$, by means of (15)-(17). All the other optical characteristics ε_λ, k_λ, $\bar{k}_\lambda$, s_λ and others we find by the methods in [1, 3].

Optical and bihemispherical thermoradiational characteristics of typical scattering capillary-porous colloidal materials were determined by the proposed method, by the graphical method and by experimental methods developed [1-3] in order to estimate the accuracy of the method and the confidence in the data, and a satisfactory converge if the quantities R_λ, T_λ, $R_{\lambda\infty}$ and L_λ is established. Thus, for a strongly scattering product, potato starch with $\lambda = 1.1$ μm the quantities $L_\lambda = 979.2$ m^{-1}, $R_{\lambda\infty} = 0.85$ were obtained by the method proposed, which differ negligibly from the experimental $R_{\lambda\infty e} = 0.86$ and calculated $L_{\lambda e} = 952.8$ m^{-1} values (relative discrepancies are $\Delta(R_{\lambda\infty}) = 1.1\%$, $\Delta(L_\lambda) = 2.1\%$).

As an illustration, data found by two methods are presented in the table for a typical comparatively weakly scattering product of grape berry flesh. As is seen from the table, the convergence of all the quantities is satisfactory, which is an indication of the reliability of the data obtained. The advantage of the analytic method is the possibility of eliminating the errors inherent in the graphical methods.

TABLE 1. Values of Optical and Bihemispherical Thermoradiational Characteristics for Grape Flesh for a λ = 1.1 μm

Method	Duntley parameters		L_λ, м$^{-1}$	$R_{\lambda\infty}$
	C_1	C_2		
Experimental analytic	0,0361	1,0897	182,0	0,289
Graphical Duntley	0,0335	1,0977	180,8	0,288

Optical characteristics are determined by using the proposed experimental-analytic method realized on an electron computer, and the radiation fields in a layer of a typical comparatively weakly scattering colloidal material from grape berries are computed in the visible and near-infrared spectrum domains 0.4-4.0 μm for solar radiation and a KG-200-1000 IR-generator radiation. The plane layer model with shell boundaries was fabricated specially from several grape berries.

The dependence of the optical characteristics of a grape berry material on the wavelength is shown in Fig. 1. As is seen, the nature of the dependence of L_λ on the wavelength is analogous to the dependence of k_λ, is much more definite. The 0.98, 1.18, 1.44, 1.93, 2.52, 2.92 μm absorption bands are explained by the presence of moisture in the grape flesh. The "backscattering" coefficient is insignificant and depends weakly on the wavelength, indicating that the grape flesh has an elongated forward-scattering index [2].

It is seen from Fig. 2a that the spectral composition of the integrated radiation varies with depth x because of the effects of selective absorption and multiple scattering. Weak absorption is observed here in the 0.7-1.4 μm spectrum range. In the 1.4-4.0 μm band where the grape flesh has higher values of the absorption coefficients, the spectral composition q'_λ and $E'_{\lambda 0}$ varies noticeably with the depth x. It should be noted that the maximal radiation energy absorption w_λ in the surface shifts for x < 1.0 mm to the longer wavelengths λ = 1.5 μm with respect to the maximum of IR-generator radiation (λ = 1.1 μm). Selective absorption results in the fact that the maximal values of the quantities w'_λ and q'_λ are shifted towards shorter wavelengths as the coordinate x increases.

Of great interest is the determination of the regularities of the radiation energy distribution of different wavelengths within the grape berry flesh layer under exposure to solar radiation. The quantities w'_λ E'_λ, q'_λ, computed by using an electronic computer for the directional exposure case are represented in Fig. 2b. It should be noted that the characteristic absorption bands near the wavelengths 0.98, 1.18, 1.44, 1.93 μm exert noticeable attenuation of the quantities w'_λ, $E'_{\lambda 0}$ and q'_λ, as is explained by the presence of narrow absorption bands in the material and in the spectral composition of solar radiation (Fig. 2b, curve 7), whose location in the sun spectrum is determined by the optical properties of the atmospheric gases)ozone, water vapor CO, etc.). It is established that the magnitude of the absorbed radiation energy in the surface layer remains high for x = 0 mm in the 0.7-0.9 and 1.4-2.6 μm wavelength bands. However, in the spectrum domain with x = 0 mm where the grape flesh has a high value of the absorption coefficient λ > 1.4 μm, a noticeable change in $\bar{k}_\lambda$ with depth x is observed.

Dependences of the quantities w_λ and $E_{\lambda 0}$ are represented in Fig. 3 in the case of bilateral exposure to a diffuse flux for each layer of a multilayer system (shell and grape flesh).

It is established that the main fraction of the radiation energy is absorbed in the surface layer in the 0.4-0.7 μm spectrum range. In the 0.7-1.4 μm wavelength band the radiation penetrates a greater depth because of the weak absorption. For λ > 1.4 the radiation is absorbed strongly and is attenuated by the material; a maximum radiation energy absorption w_λ is observed near λ = 1.5 μm. The quantify $E_{\lambda 0}$ remains high in the λ = 1.5 μm spectrum range.

Analysis of the absorbed energy distribution permits making an important practical deduction about the fact that it is expedient to use IR-generators with radiation maximum near 0.7-1.4 μm for bulk heating of a grape flesh layer. Among such generators are the KG-220-1000 type lamps.

The data obtained on the radiation spectrum fields can be utilized to compute the integrated optical characteristics of a material and the integrated radiation field distribution in a layer that are needed to determine the heat source for an analytic description of the temperature fields under IR-expose.

NOTATION

R'_λ, T'_λ $R'_{\lambda\infty}$ are directional-hemispheric $(\Theta, \varphi, 2\pi)$ thermoradiational characteristics; R_λ, T_λ, $R_{\lambda\infty}$ are bihemispherical $(2\pi; 2\pi)$ thermoradiational characteristics; L_λ, $\bar{k}_\lambda$, s_λ, ε_λ are optical characteristics-the effective attenuation, absorption "back-scattering", and extinction coefficients, m^{-1}; C_1 and C_2 are Duntley parameters, E_λ is the density of diffuse, and E'_λ the density of directional monochromatic radiation flux incident at a certain angle Θ, W/m^2; w'_λ and w_λ are the magnitudes of the absorbed radiation energy flux under directional and diffuse exposure, W/m^3; $E_\lambda{}^0$ is the magnitude of the spatial irradiance, W/m^2; and q_λ is the density of the resultant flux, W/m^2.

LITERATURE CITED

1. S. G. Il'yanov and V. V. Krasnikov, Physical Principles of Infrared Radiation of Food Products [in Russian], Moscow (1978).
2. S. G. Il'yanov, N. I. Angersbakh, and A. K. Angersbakh, Inzh.- Fiz. Zh., 51, No. 4, 633-638 (1986).
3. S. G. Il'yanov and V. V. Krasnikov, Methods of Determining the Optical and Thermal Radiation Characteristics of Food Products [in Russian], Moscow (1972).
4. G. D. Rabinovich and L. S. Slobodkin, Thermoradiation and Convective Drying of Paint and Varnish Coatings [in Russian], Minsk (1966).
5. A. P. Ivanov, Optics of Light-Scattering Medium in Physics and Biology [in Russian], Minsk (1978).
6. G. V. Rozenberg, Usp. Fiz. Nauk, 91, No. 4, 569-608 (1967).
7. É. P. Zege, M. P. Znachenok, and I. L. Katsev, Zh. Prikl. Spektr., 33, No. 4, 735-741 (1980).
8. S. Q. Duntley, JOSA, 32, No. 2, 64-70 (1942).
9. A. L. Lathrop, JOSA, 55, No. 9, 1097-1104 (1965).

HEAT TRANSFER IN ANISOTROPIC METALLIC MEDIA

V. R. Sobol' and T. A. Krivoruchko

UDC 539.22:536.2

The temperature distribution over the cross-section of a metallic sample with anisotropic kinetic coefficients heated by an electric current in liquid helium has been studied.

As is known, low-temperature phenomena of heat and charge transfer in metals are determined by the degree of nonequilibrium of the conduction electrons, their dispersion law, which results in the interaction of these phenomena, and their distinct influence on each other [1-5]. This appears to be especially strong under conditions of anisotropy, both natural, crystalline anisotropy, and also artificial anisotropy introduced, for example, by a strong external magnetic field. Thus, in metals belonging to a cubic crystallographic system, kinetic coefficients that are described by scalar values in the absence of a magnetic field become tensors of the second rank in a strong magnetic field; the latter results in the emergence of many cross effects in thermal electrotransfer.

In the present work results are given of the study of a steady-state problem of heat transfer and of the effect of the conditions for the Joule power dissipated in the volume of a sample on the temperature distribution over the cross-section of a metallic single-crystal sample in a strong transverse magnetic field with temperature-dependent kinetic coefficients of the metal.

Institute of Solid State Physics and Semiconductor Physics, Academy of Sciences of the Belorussian SSR, Minsk.

Translated from Inzhenerno-Fizicheskii Zhurnal, Vol. 58, No. 4, pp. 670-675, April, 1990. Original article submitted January 23, 1989.

0022-0841/90/5804-0514$12.50